the octahedral sites of the talc layer are thus available to divalent ions, but the number of divalent ions in the brucite layer is limited, with the rest of the octahedral positions filled with trivalent ions. The excess positive charge which is thus imparted to the brucite layer neutralizes the charge on the talc layer in the same manner as the potassium ion in the mica structure. In the oxidized chlorite specimen, however, the charge distribution will be altered because most of the ferrous iron will become trivalent and part of the excess negative charge in the talc layer is now compensated by the increased positive charge on the octahedral talc layer. A possible mechanism for keeping the structure neutral would be for some of the hydroxyl groups of the brucite layer to lose hydrogen ions. Thus weathering of a high-iron chlorite could lead to a preferential attack on the brucite layer and subsequently produce other types of clay minerals.

References

BRINDLEY, G. W., OUGHTON, B. M. & ROBINSON, K. (1950). *Acta Cryst.* **3**, 408.

CLARKE, F. W. & SCHNEIDER, E. A. (1891). *Bull. U.S. Geol. Surv.* **78**, 19.

MCMURCHY, R. C. (1934). *Z. Kristallogr.* **88**, 420.

PAULING, L. (1930). *Proc. Nat. Acad. Sci. U.S.* **16**, 578.

SMITH, J. V. (1954). *Acta Cryst.* **7**, 479.

Acta Cryst. (1958). **11**, 195

The Crystal Structure of Chlorite. II. A Triclinic Polymorph*

BY HUGO STEINFINK

Shell Development Company Exploration and Production Research Division, Houston, Texas, U.S.A.

(*Received* 13 *June* 1957 *and in revised form* 14 *October* 1957)

The crystal structure of the triclinic chlorite corundophillite differs from the monoclinic polymorph prochlorite in the stacking of the two Si–O layers in the talc portion of the structure. Shifting of the SiO_4 tetrahedra away from their ideal positions occurs also in this structure. The isomorphous substitution occurs at random in this structure. The brucite layer is held to the talc layer by hydrogen bonds, which are 2·92 Å long. The neutralization of the charge arising in the tetrahedral layer is compensated by isomorphous substitution in the octahedral positions of both the talc and brucite layers.

Introduction

The analysis of the structure of a chlorite in Part I (Steinfink, 1958) has confirmed the *L* structure postulated for it by Brindley, Oughton & Robinson (1950), but in addition has demonstrated that a rotation of the Si–O tetrahedra, together with other deviations from the ideal coordinates, exist. It has also shown a rather high degree of ordering of cations which replace the magnesium and silicon ions in the octahedral and tetrahedral sites respectively. The structural investigation of a triclinic polymorph with a composition very close to that of an 'ideal' chlorite should thus provide information about the influence of isomorphous substitution on ordering and on the extent of deviation of atomic parameters from their ideal values.

Experimental determination of the structure

The single-crystal diffraction data for the structure determination of the triclinic polymorph were collected from a chlorite specimen obtained from the Harvard University collection. It was labeled 'Corundophillite from the Mochako District, Kenya'. The chemical analysis obtained in this laboratory is shown in Table 1 and the chemical formula, based on this analysis and assuming 10 oxygen atoms per formula unit, is

$$(Mg_{4\cdot9}Al_{0\cdot75}Fe'''_{0\cdot17}Fe''_{0\cdot07}Cr'''_{0\cdot18})(Si_{2\cdot6}Al_{1\cdot4})O_{10}(OH_8)\ .$$

Table 1. *Analysis*

Constituent	%
SiO_2	27·4
Fe_2O_3	2·4
FeO	0·8
Al_2O_3	18·9
Cr_2O_3	2·3
MgO	34·0

The optic sign of this sample of chlorite is (+): $2V = 44° 45'$, and was measured on the universal stage by the direct method; both n_X and n_Y lie

---

* Publication No. 134.

between 1·5775 and 1·5885 with the probable value of $n_X = 1{\cdot}580$ and the probable value of $n_Y = 1{\cdot}585$.*

X-ray diffraction data from a single crystal with dimensions approximately $0{\cdot}1 \times 0{\cdot}15 \times 0{\cdot}05$ mm. were collected with both Weissenberg and precession cameras, using Cu $K\alpha$ and Mo $K\alpha$ radiations respectively. The unit-cell dimensions are

$$a = 5{\cdot}34,\ b = 9{\cdot}27,\ c = 14{\cdot}36\ \text{Å, all } \pm 0{\cdot}02\ \text{Å},$$
$$\beta = 97^\circ\ 22' \pm 6' .$$

The space group is $C1$ and there are two 'molecules' in the unit cell. The calculated density is 2·71 g.cm.$^{-3}$ as compared with the observed density 2·71 g.cm.$^{-3}$.

The ideal coordinates for the triclinic *M* structure (Brindley *et al.*, 1950) were used to compute phases for a (0*kl*) Fourier projection. Although this projection does not resolve the oxygen atoms of the base of the Si–O tetrahedron, it was constructed primarily to see whether iron and chromium atoms tend to occupy preferentially any particular octahedral position in either the talc or brucite layer. The projection (Fig. 1) showed all octahedral peaks to be of the same height with no preferential position, and an average scattering power of $\frac{1}{6}(\mathrm{Mg}_{5\cdot0}\mathrm{Fe}_{0\cdot4}\mathrm{Al}_{0\cdot6})$ in octahedral positions was used in the further refinement of the structure.

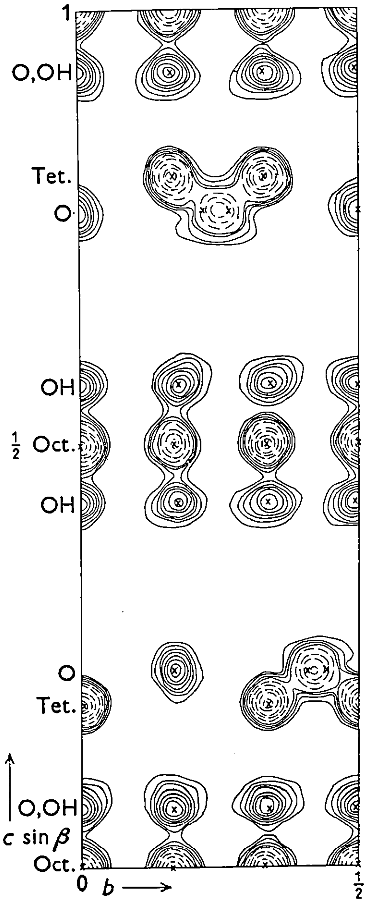

Fig. 1. The (0*kl*) electron-density projection of corundophillite. Contours in intervals of approximately 2 e.Å^{-2}, beginning at 4 e.Å^{-2}. The broken contours are in intervals of 5 e.Å^{-2}. Crosses mark the final locations of the atoms.

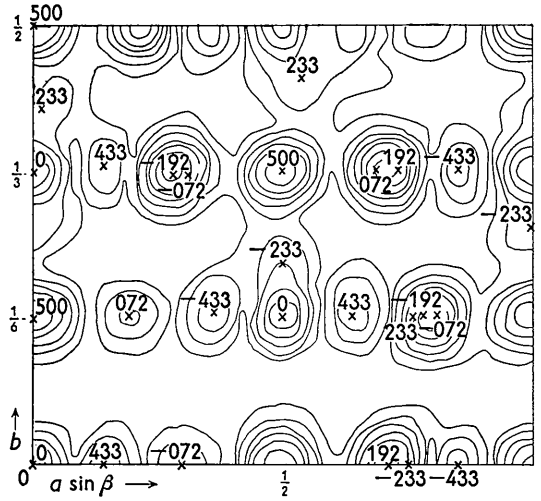

Fig. 2. The (*hk*0) electron-density projection of corundophillite. Contours in approximately 10 e.Å^{-2} intervals, beginning at 10 e.Å^{-2}. Crosses mark the final locations of the atoms and the numbers give the value of the *z* parameter of the atom in units of *c*/1000.

Table 2. *Atomic coordinates for the triclinic polymorph, corundophillite*

Atom	*x*	*y*	*z*
$\frac{1}{6}(\mathrm{Mg}_{5\cdot0}\mathrm{Fe}_{0\cdot4}\mathrm{Al}_{0\cdot6})$	0	0	0
	0	0·333	0
	0	0·667	0
	0	0·167	0·500
	0	0·500	0·500
	0	0·833	0·500
$\frac{1}{4}(\mathrm{Si}_{2\cdot5}\mathrm{Al}_{1\cdot5})$	0·270	0·332	−0·192
	0·770	0·168	−0·192
	0·237	0·503	0·192
	0·735	0·337	0·192
O	0·010	0·406	0·233
	0·530	0·443	0·233
	0·710	0·168	0·233
	0·990	0·268	−0·233
	0·490	0·230	−0·233
	0·803	0	−0·233
	0·690	−0·002	0·072
	0·690	0·668	0·072
	0·690	0·336	0·072
	0·298	−0·004	−0·072
	0·310	0·330	−0·072
	0·810	0·167	−0·072
	0·144	−0·007	0·433
	0·143	0·673	0·433
	0·140	0·335	0·433
	0·851	−0·004	−0·433
	0·858	0·676	−0·433
	0·857	0·340	−0·433

---

* The optical properties were obtained through the cooperation of M. Friedman of Shell Development Company, E. and P. Research Laboratory.

Table 3. *Calculated and observed structure factors*

h	k	l	$\|F_c\|$	F_o
0	2	0	38	38
	4		21	23
	6		189	182
1	1	0	63	65
	3		38	42
	5		44	43
	7		36	40
	11		12	12
2	0	0	2	-
	2		5	-
	4		25	32
	6		29	27
3	1	0	47	35
	3		14	17
	5		17	20
	7		13	-
	9		5	-
4	0	0	98	102
	2		7	17
	4		4	-
	6		47	52
5	1	0	15	17
	3		23	28
	7		15	13
6	0	0	33	30
$\bar{1}$	1	0	55	48
	3		25	35
	5		33	33
	7		10	-
	11		14	13
$\bar{2}$	2	0	14	-
	4		15	22
	6		32	27
$\bar{3}$	1	0	18	22
	3		13	-
	5		33	27
	7		10	13
	9		2	12
$\bar{4}$	2	0	18	17
	4		3	13
	6		42	53
$\bar{5}$	1	0	4	-
	3		25	27
	7		1	-
0	0	1	45	40
		2	99	94
		3	114	117
		4	176	152
		5	100	110
		6	12	32
		7	72	88
		8	26	25
		9	32	50
		10	69	80
		12	68	70
		14	57	63
		16	62	60
2	0	1	131	137
		2	92	94
		3	22	23
		4	15	142
		5	102	82
		6	67	55
		7	29	32
		8	155	130
		9	55	48
		12	33	32
		13	35	37
		14	21	24
		15	23	32
		17	9	16
		18	28	48

h	k	l	$\|F_c\|$	F_o
4	0	1	76	79
		2	21	23
		4	70	68
		5	49	40
		6	77	70
		7	31	35
		8	25	24
		9	30	32
		10	37	43
		12	21	28
		15	10	20
6	0	1	25	33
		2	17	27
		3	22	28
		4	24	28
		5	13	23
		6	18	20
		8	32	56
		9	12	22
$\bar{2}$	0	1	28	28
		2	98	98
		3	122	133
		4	85	94
		5	53	49
		6	87	92
		7	49	41
		8	151	134
		9	15	24
		10	36	32
		11	78	78
		12	58	70
		13	10	21
		14	36	43
		15	25	24
		17	22	37
		18	36	55
		19	18	25
$\bar{4}$	0	1	7	-
		2	28	31
		3	62	59
		4	87	85
		6	57	51
		7	64	63
		8	55	64
		9	25	35
		10	78	80
		11	22	25
		12	21	24
		14	15	23
		15	14	16
		16	17	29
$\bar{6}$	0	1	14	15
		2	68	74
		4	33	37
		6	25	31
		8	17	25
		12	19	36
		13	17	25
0	2	1	55	60
		2	54	49
		3	16	16
		4	53	56
		5	15	16
		6	36	36
		7	25	32
		9	22	24
		10	11	16
		11	4	12
		12	13	16
		13	9	16
		14	7	12
		15	14	12
		17	11	12
		18	13	12

h	k	l	$\|F_c\|$	F_o
0	4	1	14	16
		2	21	24
		3	24	20
		4	34	32
		5	40	44
		6	32	36
		7	47	44
		9	54	56
		11	42	40
		12	26	28
		13	23	24
		14	34	28
		16	25	24
		18	17	16
0	6	1	20	20
		2	95	83
		3	52	44
		4	64	60
		5	47	48
		6	46	52
		7	23	32
		8	36	24
		10	84	83
		11	38	40
		12	56	56
		13	33	36
		14	67	64
		15	23	24
		16	78	75
		17	13	20
0	8	2	8	12
		3	16	12
		4	5	12
		5	27	24
		7	24	24
		8	24	16
		9	22	24
		10	28	23
		12	25	24
		13	11	12
		14	24	24
		15	14	12
0	10	1	15	20
		3	12	20
		4	10	12
		6	17	24
		9	14	20
		11	12	16
0	12	0	97	107
		2	22	20
		3	23	24
		4	37	40
		5	26	24
		6	14	20
		7	20	40
0	$\bar{2}$	1	68	60
		2	9	8
		3	60	64
		4	32	32
		5	31	36
		6	36	32
		8	30	28
		9	15	16
		10	5	12
		11	16	16
		12	9	16
		14	12	12
		16	9	12
		17	13	12
		19	12	16

h	k	l	$\|F_c\|$	F_o
0	$\bar{4}$	1	28	32
		3	35	40
		4	12	12
		5	42	40
		6	36	36
		7	39	44
		8	40	32
		9	17	20
		10	50	52
		12	43	40
		13	18	20
		14	24	24
		15	27	24
		16	12	12
		17	22	24
0	$\bar{6}$	1	20	32
		2	107	111
		3	51	56
		4	69	64
		5	39	44
		6	52	60
		7	21	20
		9	36	32
		10	73	75
		11	43	44
		12	58	67
		13	32	36
		14	60	60
		15	21	20
		16	84	75
		17	9	12
0	$\bar{8}$	2	17	16
		4	18	24
		6	13	16
		7	30	28
		9	28	24
		10	15	12
		11	25	24
		12	22	24
		13	14	16
		14	21	16
0	$\overline{10}$	2	18	20
		4	14	16
		7	18	20
		10	13	16
		12	14	12
		13	5	8
0	$\overline{12}$	1	15	20
		2	32	28
		3	29	28
		4	37	32
		5	25	24
		6	23	24
		7	17	16
1	$\bar{9}$	1	41	40
	$\bar{7}$		35	35
	$\bar{5}$		10	8
	$\bar{3}$		100	103
	$\bar{1}$		55	49
	1		15	23
	3		101	120
	5		15	15
	9		48	52
	11		14	12
$\bar{1}$	$\bar{1}$	1	46	37
	1		27	16
	5		39	35
	7		22	20

h	k	l	$\|F_c\|$	F_c
2	$\bar{8}$	1	18	16
	$\bar{6}$		62	60
	$\bar{4}$		30	28
	$\bar{2}$		17	20
	2		29	23
	4		29	28
	6		58	63
$\bar{2}$	$\bar{4}$	1	18	24
	$\bar{2}$		17	24
	2		18	15
	4		43	41
3	$\bar{9}$	1	31	31
	$\bar{7}$		13	13
	$\bar{5}$		18	19
	$\bar{3}$		87	91
	$\bar{1}$		39	36
	1		13	16
	3		79	85
	5		35	29
	9		29	32
$\bar{3}$	$\bar{9}$	1	65	53
	$\bar{5}$		34	27
	$\bar{3}$		192	143
	1		29	23
	3		190	171
	9		69	75
4	$\bar{6}$	1	49	51
	$\bar{2}$		25	23
	2		20	20
	6		50	49
$\bar{4}$	$\bar{2}$	1	35	21
	2		21	20
	4		2	16
5	$\bar{7}$	1	14	15
	$\bar{3}$		45	52
	$\bar{1}$		19	17
	1		8	13
	3		46	49
	5		10	13
	7		8	9
$\bar{5}$	7	1	12	16
6	$\bar{4}$	1	9	11
	$\bar{2}$		3	11
	2		3	9
	4		8	19
$\bar{6}$	4	1	12	15

In order to check the x, y parameters an ($hk0$) projection (Fig. 2) was evaluated. In spite of the large amount of overlap encountered in this view of the structure, it nevertheless showed the hydroxyl groups of the brucite layer in almost ideal positions as opposed to the rather large shift observed in the monoclinic polymorph. No definite x, y parameters could be obtained for the basal oxygen atoms because of the overlap.

An increase in the resolution of a projection can frequently be achieved by constructing the functions $C_L(x, y)$, $S_L(x, y)$, and $|\varrho_L(x, y)|$ (Phillips, 1954). The function $|\varrho_1(x, y)|$ obtained with ($hk1$) data is shown in Fig. 3, and, compared with the ($hk0$) projection (Fig. 2), indicates a considerable increase in the resolution of the atoms. The final x, y parameters were obtained by this method, and the atomic coordinates for the structure are shown in Table 2.

The discrepancy coefficient $R(hk0)$ is 0·133, $R(hk1)$ is 0·147, $R(h0l)$ is 0·146, and $R(0kl)$ is 0·121. Only observed structure factors are included in the computation of R. Weighted scattering factors as shown in Table 2 were used for the octahedral and tetrahedral positions; an isotropic temperature factor was evaluated separately for these zones and was found to be 2·25 Å^2 for $hk0$, $hk1$, and $h0l$, and 0·72 Å^2 for $0kl$. Calculated and observed values of F are listed in Table 3.

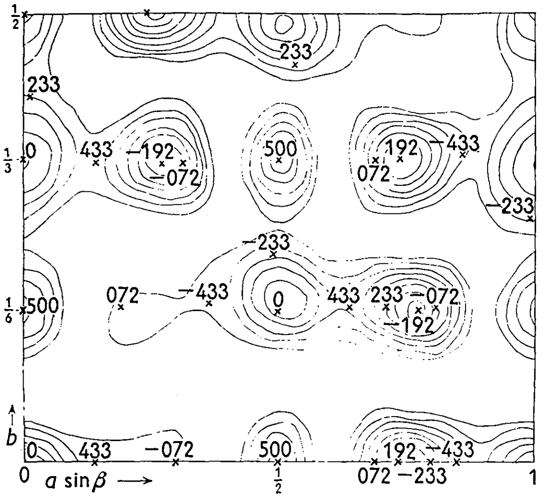

Fig. 3. The (*hkl*) generalized projection. Contours in approximately 4 e.Å^{-2} intervals, beginning at 4 e.Å^{-2}.

Discussion

The results of the investigations reported in Part I and in this paper confirm that the polymorphism of the chlorites with unit cells whose *c* axis is approximately 14 Å is due to the different arrangements of the two Si–O nets relative to each other within the talc layer (Brindley *et al.*, 1950). Table 4 shows that a rotation of the SiO_4 tetrahedra occurs in this structure as well as in the monoclinic polymorph. A similar rotation has also been observed in related structures such as amesite (Steinfink & Brunton, 1956) and also in dickite (Newnham & Brindley, 1956). The rotations of the SiO_4 tetrahedra in this and similar structures must result from the attempt of two layers with different fundamental translations, the Mg–O octahedral and the Si–O tetrahedral layer, to come into concordance. The extent of isomorphous substitution in the structure determines the linear expansion of one layer with respect to the other so that the amount of distortional adjustment to bring about a better fit between the two layers should be dependent on such substitution. A direct comparison between the shifts occurring in the two polymorphs shows that distortion from the ideal parameters is less in the triclinic case. Both polymorphs contain approximately the same amount of aluminum in tetrahedral position but differ appreciably in the amounts of iron in the octahedral talc positions. It is quite probable that the iron was in the ferrous state in the unoxidized minerals, so that the dimensions of the octahedral talc layer in the monoclinic polymorph are larger than in the triclinic structure, and the tetrahedral layer has to undergo a larger distortion to fit itself to its octahedral neighbor. The larger value of b_0 in prochlorite also reflects this expansion of the octahedral talc layer. The increase in the dimension of the tetrahedral layer can be accomplished more easily when aluminum goes into definite tetrahedral sites rather than be distributed randomly, because of the larger value of a Al–O bond length over the length of a (Si, Al)–O bond. Thus the localization of aluminum into specific sites in the monoclinic prochlorite probably results from the high iron substitution in that structure, while the random aluminum distribution in the triclinic corundophillite is consistent with the lesser octahedral substitution.

Table 4. *Changes in the x, y parameters of the basal oxygen ions in corundophillite*

Brindley			This paper		
x	*y*	*z*	*x*	*y*	*z*
−0·006	0·917	0·233	0·030	0·943	0·233
−0·006	0·417	0·233	0·010	0·406	0·233
0·244	0·667	0·233	0·210	0·668	0·233
0·755	0	−0·233	0·803	0	−0·233
0·005	0·750	−0·233	−0·010	0·730	−0·233
0·005	0·250	−0·233	−0·010	0·268	−0·233

The average of the twelve independent Si–O distances is $1{\cdot}66 \pm 0{\cdot}01_6$ Å, and if use is made of the curve published by Smith (1954), a 33% substitution of aluminum for silicon is obtained. This agrees very well with the value of 35% obtained from the chemical analysis. The bond length between silicon and the oxygen which is also bonded to magnesium is 1·71 Å, the same value found for this bond in the monoclinic variety. The average bond length for Mg–O is 2·05±0·02 Å; the O–Si–O angle is tetrahedral, and the Si–O–Si angle is 135°. The hydroxyls of the brucite layer form a hydrogen bond with the oxygens of the talc layer, whose average length is 2·92 Å.

I wish to thank Dr W. F. Bradley and Dr R. A. Rowland for their critical reviews of the manuscripts and for many stimulating discussions, and to acknowledge the help of Mr F. J. Sans, who selected the crystals and took the diffraction photographs.

References

Brindley, G. W., Oughton, B. M. & Robinson, K. (1950). *Acta Cryst.* **3**, 408.
Newnham, R. E. & Brindley, G. W. (1956). *Acta Cryst.* **9**, 759.
Phillips, D. C. (1954). *Acta Cryst.* **7**, 221.
Smith, J. V. (1954). *Acta Cryst.* **7**, 479.
Steinfink, H. (1958). *Acta Cryst.* **11**, 191.
Steinfink, H. & Brunton, G. (1956). *Acta Cryst.* **9**, 487.